Supplement of Hydrol. Earth Syst. Sci., 29, 5299–5313, 2025 https://doi.org/10.5194/hess-29-5299-2025-supplement © Author(s) 2025. CC BY 4.0 License.





### Supplement of

# Dynamic assessment of rainfall erosivity in Europe: evaluation of EURADCLIM ground-radar data

Francis Matthews et al.

Correspondence to: Nejc Bezak (nejc.bezak@fgg.uni-lj.si)

The copyright of individual parts of the supplement might differ from the article licence.

## Supplement to: Dynamic assessment of rainfall erosivity in Europe: evaluation of EURADCLIM ground-radar data

#### Rainfall erosivity calculations

For each grid cell covered by EURADCLIM, 30 min precipitation time series were obtained based on the best performing disaggregation scheme. The erosive events for each grid cell were then defined according to the procedure described in the RUSLE handbook (Renard et al., 1997). Thus, two events were separated in case of less than 1.27 mm of rain within a continuous 6-hour period. Only erosive rainfall events with more than 12.7 mm of rainfall in total, or 6.35 mm in 15 minutes (30 minutes due to time step used), were used in the rainfall erosivity calculations (Renard et al., 1997). Smaller events below these limits were discarded from the calculations. To calculate the specific kinetic energy  $e_B$  (MJ ha<sup>-1</sup> mm<sup>-1</sup>) the Brown and Foster (1987) equation was used:

$$e_B = 0.29 \cdot [1 - 0.72 \cdot \exp(-0.05 \cdot i)],$$
 (S1)

where i is rainfall intensity (mm  $h^{-1}$ ). In order to derive the average annual rainfall erosivity (R-factor) (MJ mm  $ha^{-1}h^{-1}$ ), the following two equations were applied (Renard et al., 1997):

$$E = e_B \cdot i \cdot \Delta t, \tag{S2}$$

$$R = \frac{\sum_{n} E \cdot I_{30}}{N},\tag{S3}$$

where E is the kinetic energy of the individual erosive event (MJ ha<sup>-1</sup>),  $\Delta t$  is the time interval, and I30 is the maximum 30-minute rainfall intensity (mm h<sup>-1</sup>) of the erosive event n, which occurred within a time span of N years. This procedure was applied for all grid cells covered by the EURADCLIM product to give both time series of EI30 and the average annual R-factor. The R code (R Core Team, 2021) for calculating rainfall erosivity developed by (Pidoto et al., 2022) was used in this study.

### REFERENCES

Brown, L. C. and Foster, G.: Storm erosivity using idealised intensity distribution, T. ASAE, 30, 379–386, https://doi.org/10.13031/2013.31957, 1987.

Pidoto, R., Bezak, N., Müller-Thomy, H., Shehu, B., Callau-Beyer, A. C., Zabret, K., and Haberlandt, U.: Comparison of rainfall generators with regionalisation for the estimation of rainfall erosivity at ungauged sites, Earth Surface Dynamics, 10, 851–863, https://doi.org/10.5194/esurf-10-851-2022, 2022.

R Core Team: R: A Language and Environment for Statistical Computing, https://www.r-project.org/, 2021.

Renard, K. G., Foster, G. R., Weesies, G. A., McCool, D. K., and Yoder, D. C.: Predicting Soil Erosion by Water: A Guide to Conservation Planning with the Revised Universal Soil Loss Equation (RUSLE) (Agricultural Handbook 703), US Department of Agriculture, ISBN 0-16-048938-5, 1997.

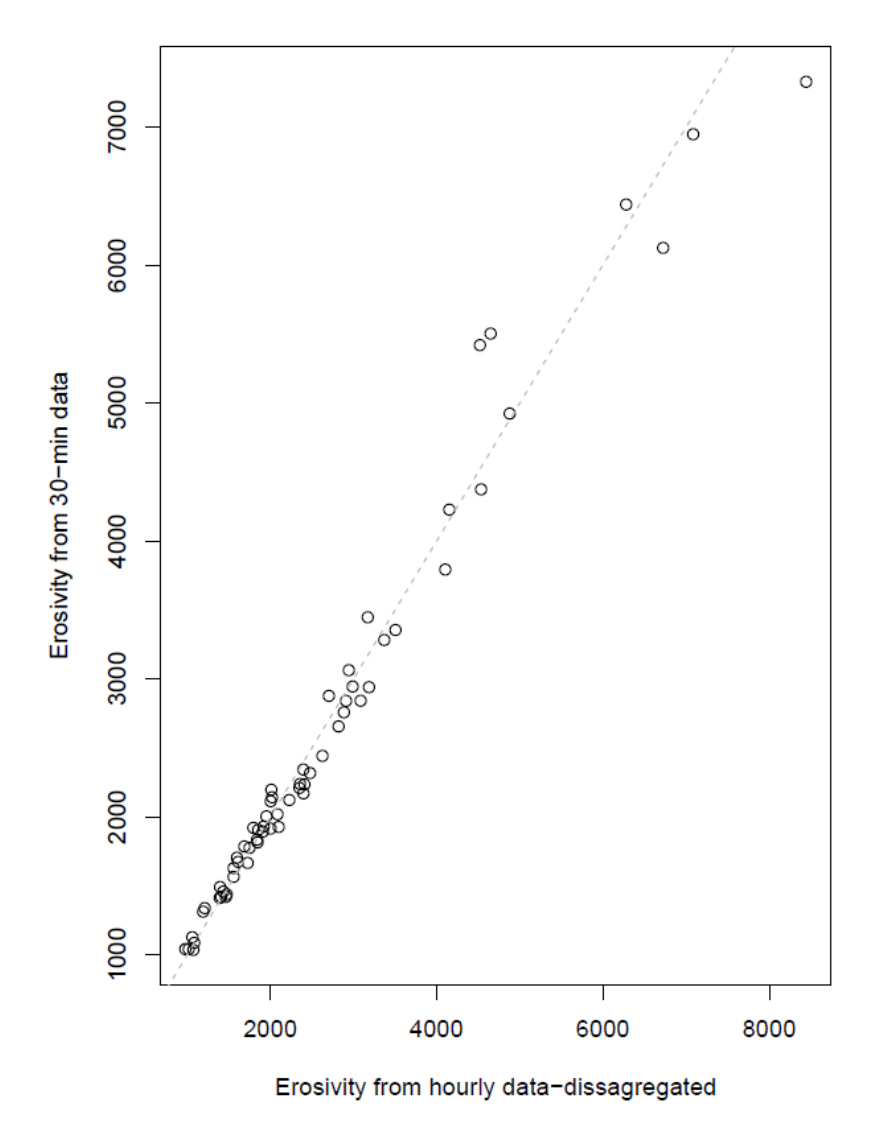


Figure S1: Comparison between rainfall erosivity calculated based on the 30-min rainfall data and based on the rainfall erosivity calculated based on the disaggregated rainfall data (i.e., where 25 % of rainfall was considered in first 30-min and 75 % of rainfall in second 30-min).

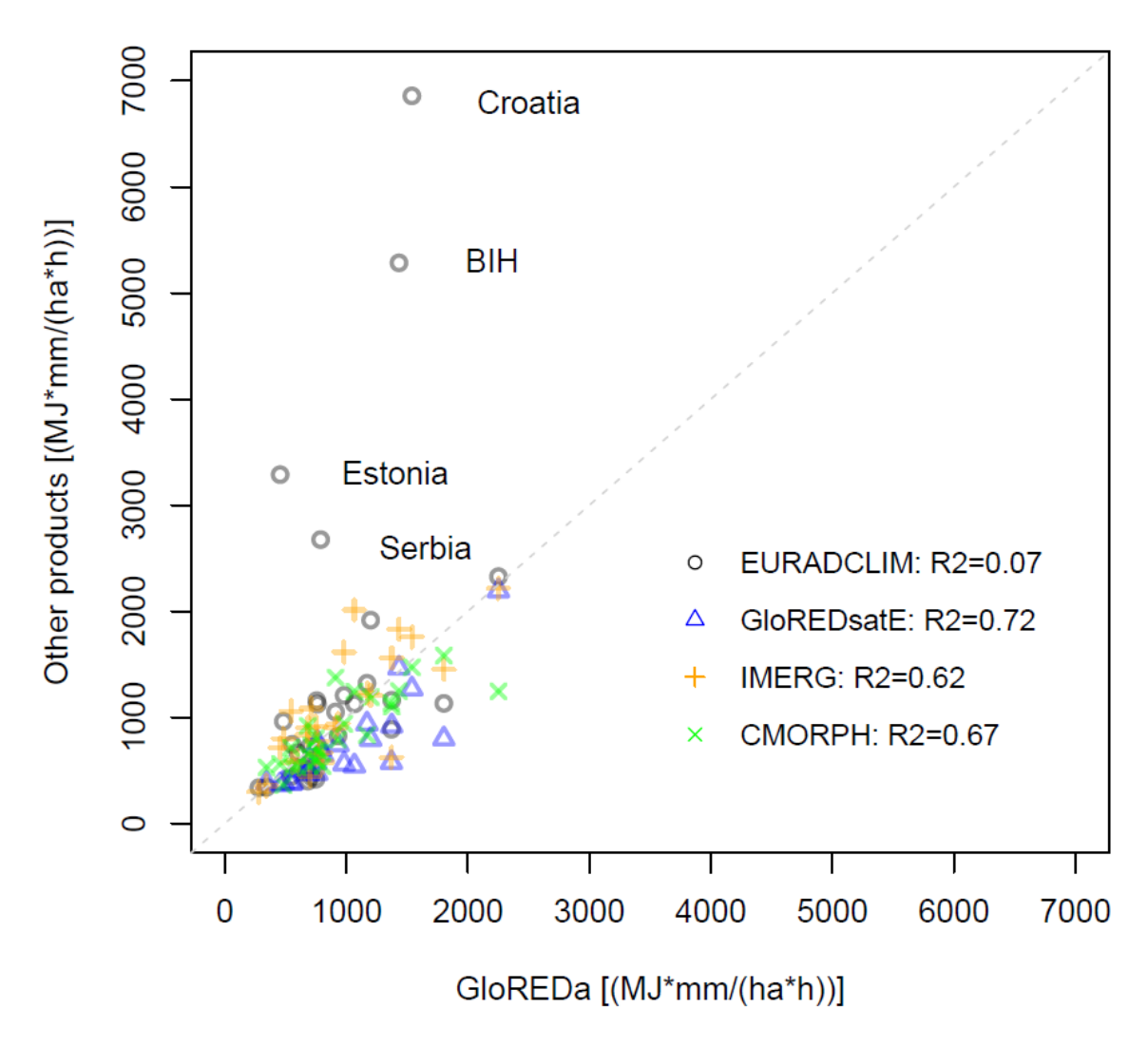


Figure S2: Comparison between annual rainfall erosivity for GloREDa (Panagos et al., 2023), EURADCLIM (this study), GloREDsatE (Das et al., 2024), IMERG (Das et al., 2024) and CMORPH (Bezak et al., 2022). Only European countries (country-average values were used) covered by EURADCLIM are shown. BIH stands for Bosnia and Herzegovina.

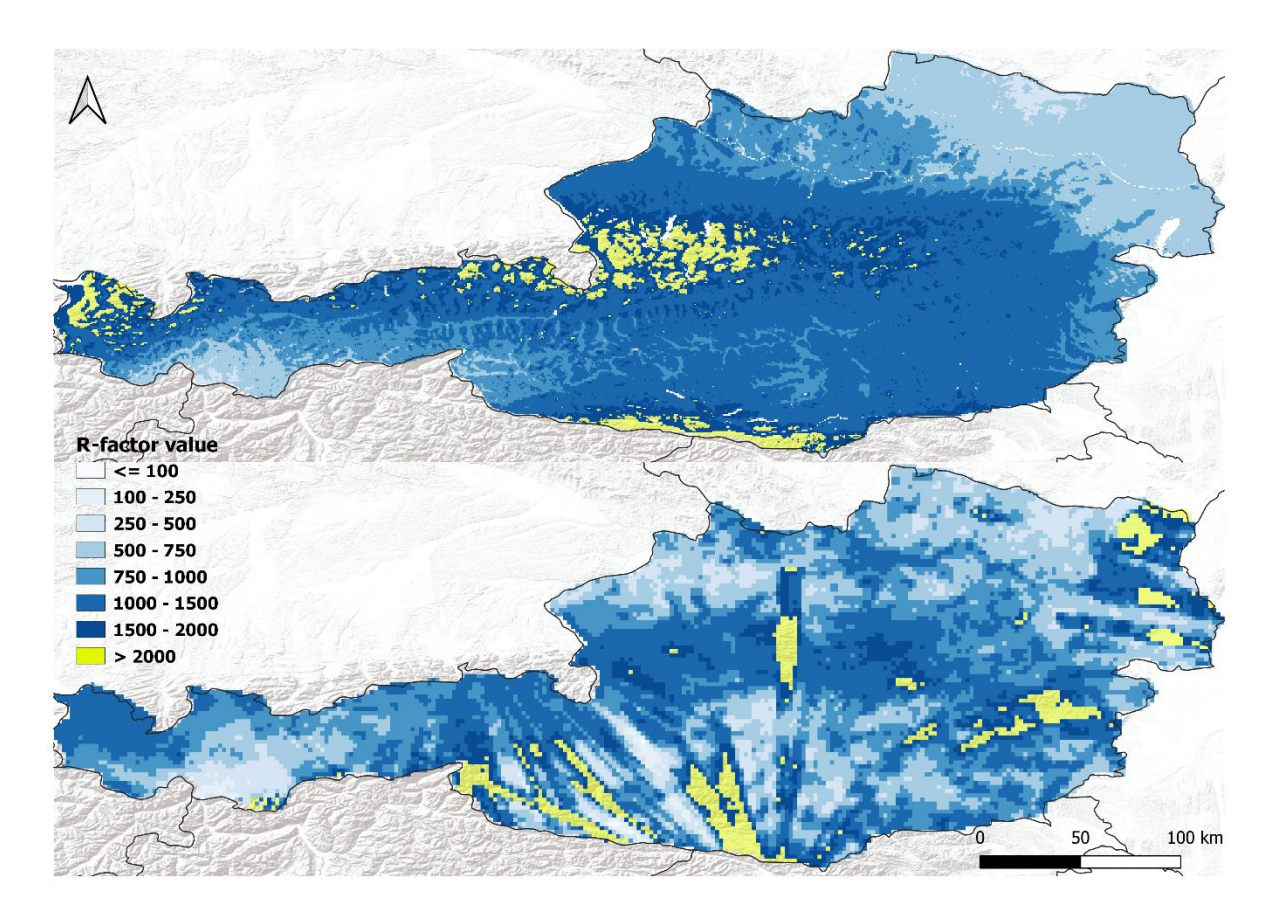


Figure S3: Comparison between the average annual rainfall erosivity (MJ mm ha<sup>-1</sup> h<sup>-1</sup>) for Austria derived based on the GloREDa (upper) and EURADCLIM (lower) predictions. Linear features represent the propagation of artefacts into the unadjusted EURADCLIM-derived rainfall erosivity. It should be noted that Austrian radars did not contribute to the OPERA data used in EURADCLIM, therefore the ground radar coverage comes from neighboring countries causing a consequent reduction in data quality for long distance retrievals.

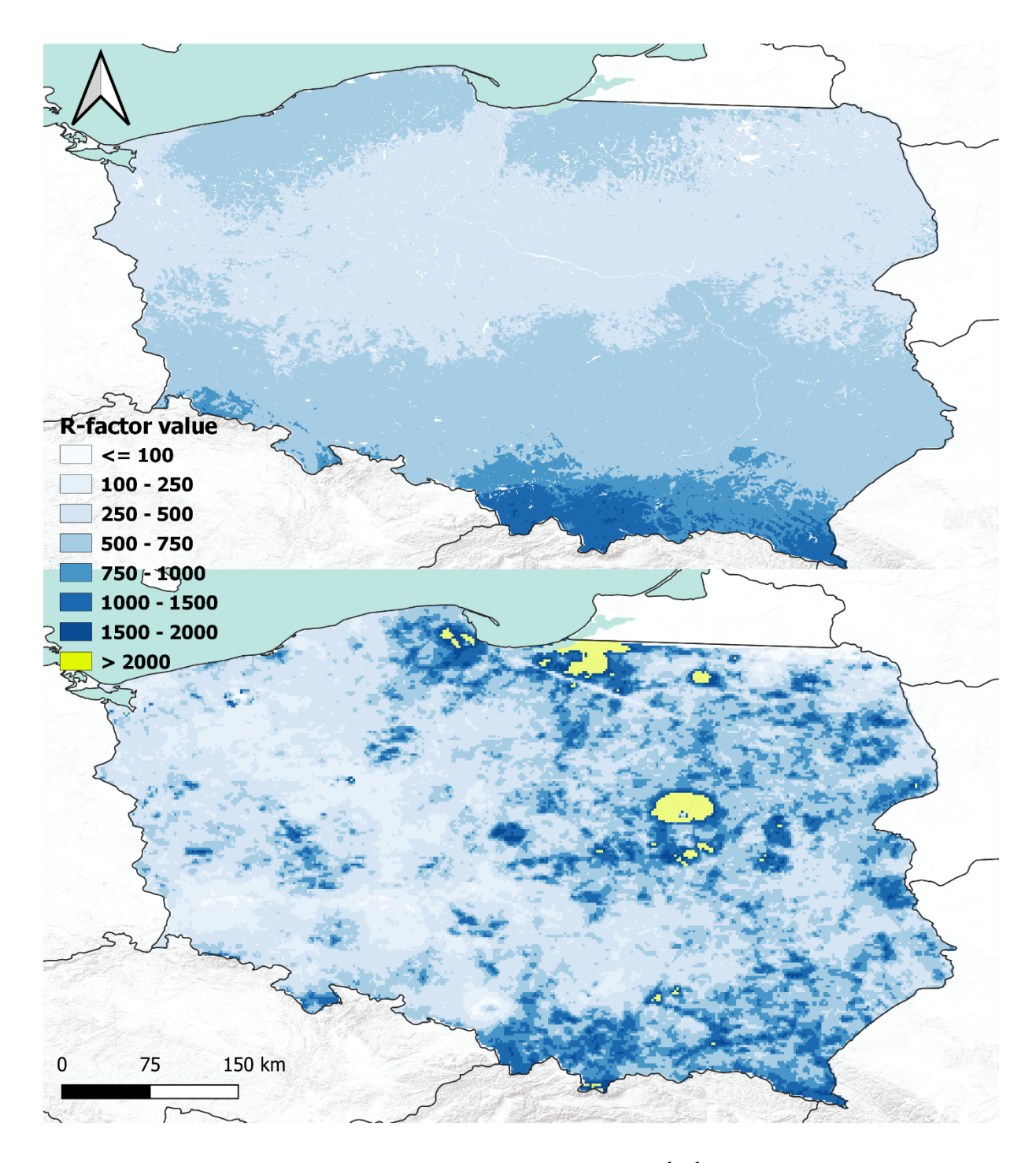


Figure S4: Comparison between annual rainfall erosivity (MJ mm  $ha^{-1} h^{-1}$ ) for Poland derived based on the EURADCLIM (lower) and GloREDa (upper) datasets.

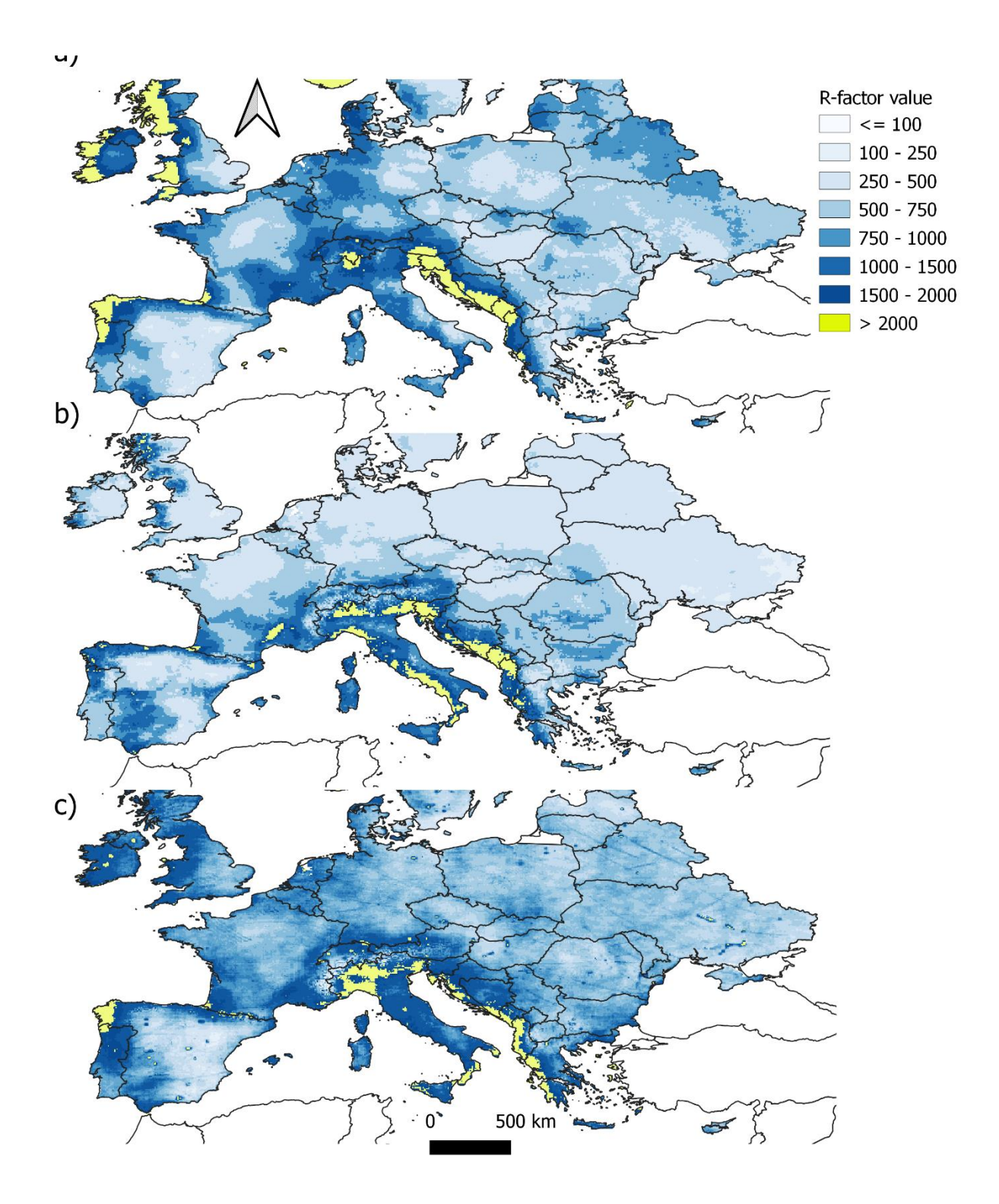


Figure S5: Comparison between rainfall erosivity (R) (MJ mm ha $^{-1}$  h $^{-1}$ ) calculated using IMERG dataset (a), GloRESatE dataset (b) and CMORPH (c) for Europe. Maps a) and b) are adopted after Das et al. (2024). Map c) is adopted after Bezak et al. (2022).

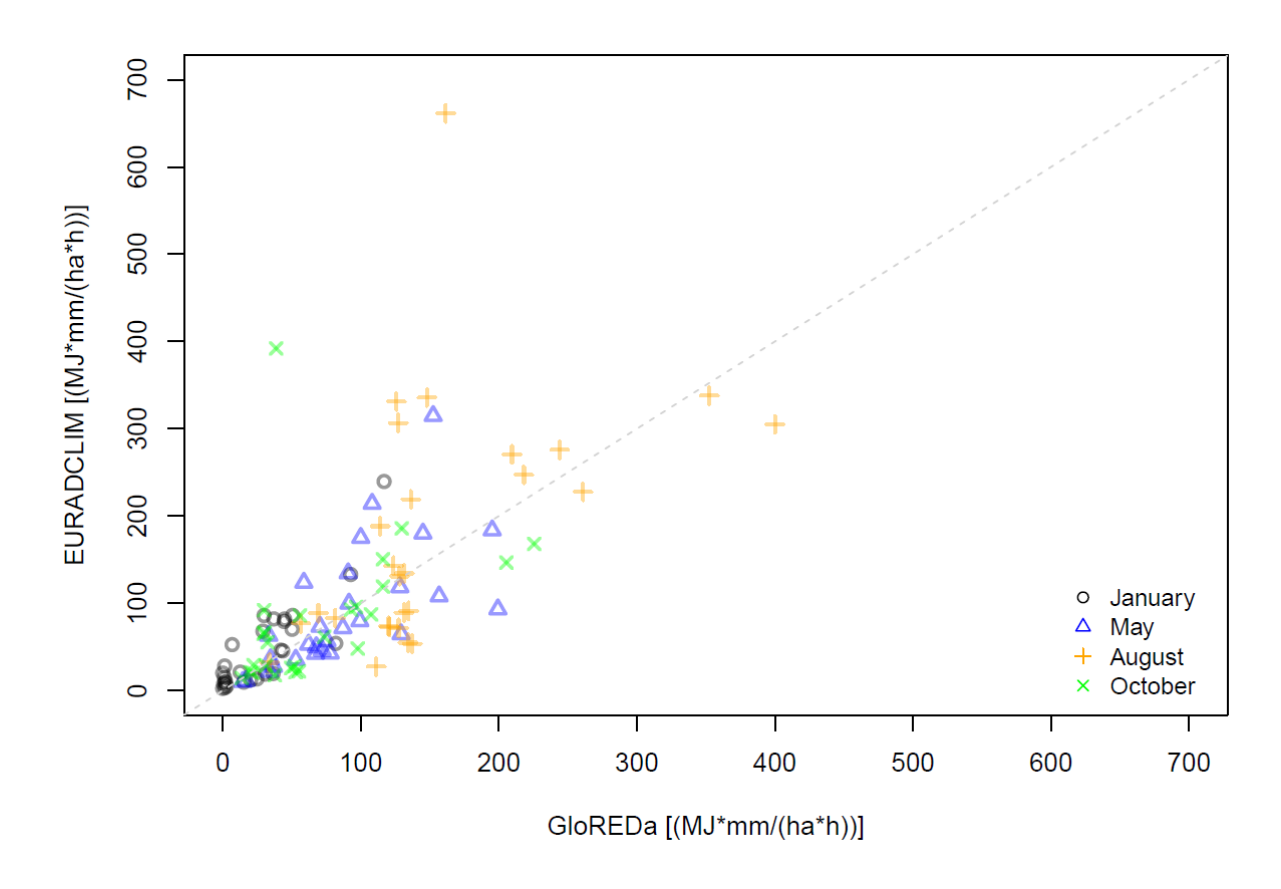


Figure S6: Comparison between monthly rainfall erosivity for January, May, August and October based on the EURADCLIM (x-axis) and GloREDa (y-axis) datasets.

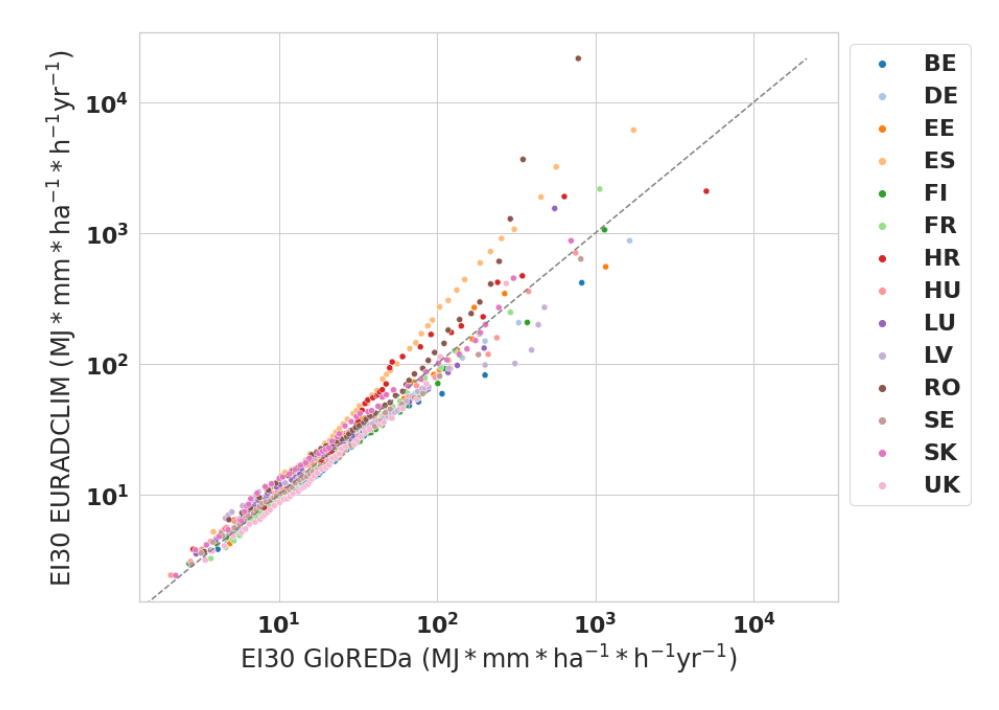


Figure S7: Quantile-Quantile plot between GloREDa (rain gauges) and EURADCLIM (gridded estimates) EI30 events for the year 2013, giving a grid-to-point comparison of the predicted and measured EI30 values. Points are coloured based on the country. It should be noted that both x and y axis are shown in log-scale.

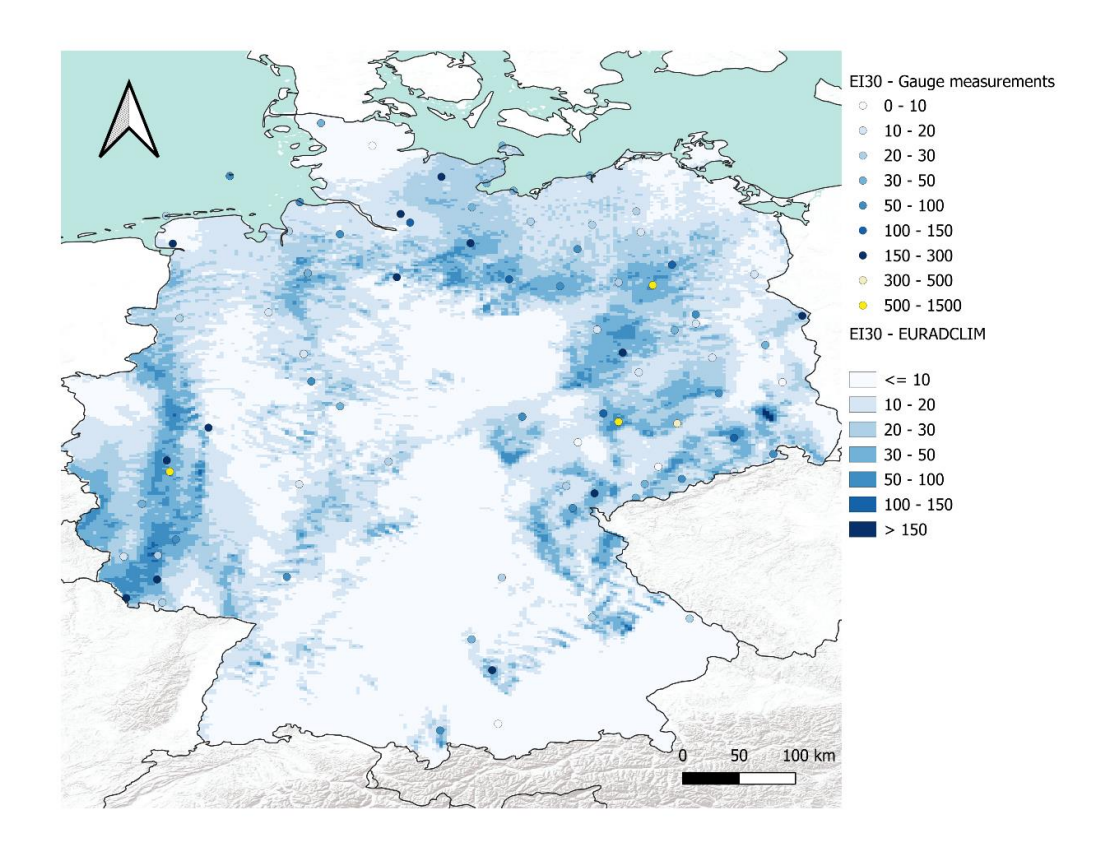


Figure S8: Comparison between spatial rainfall erosivity (EI30) patterns detected by EURADCLIM for the event that occurred on the 20<sup>th</sup> of June 2013 and the corresponding GloREDa station measurements.

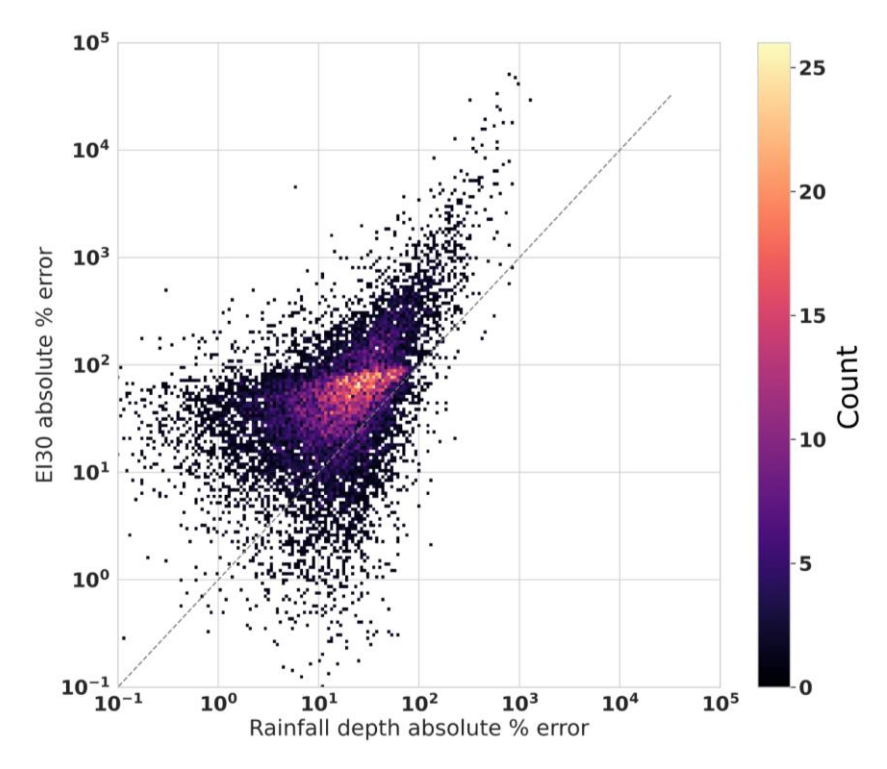


Figure S9: A comparison between the absolute % error between the event rainfall depth predictions by EURADCLIM and the computed EI30 value. The central dotted line depicts an equal ratio of relative error on the rainfall depth predictions to the error on the EI30, while values above and below represent error inflation and deflation in the consequent prediction of EI30.

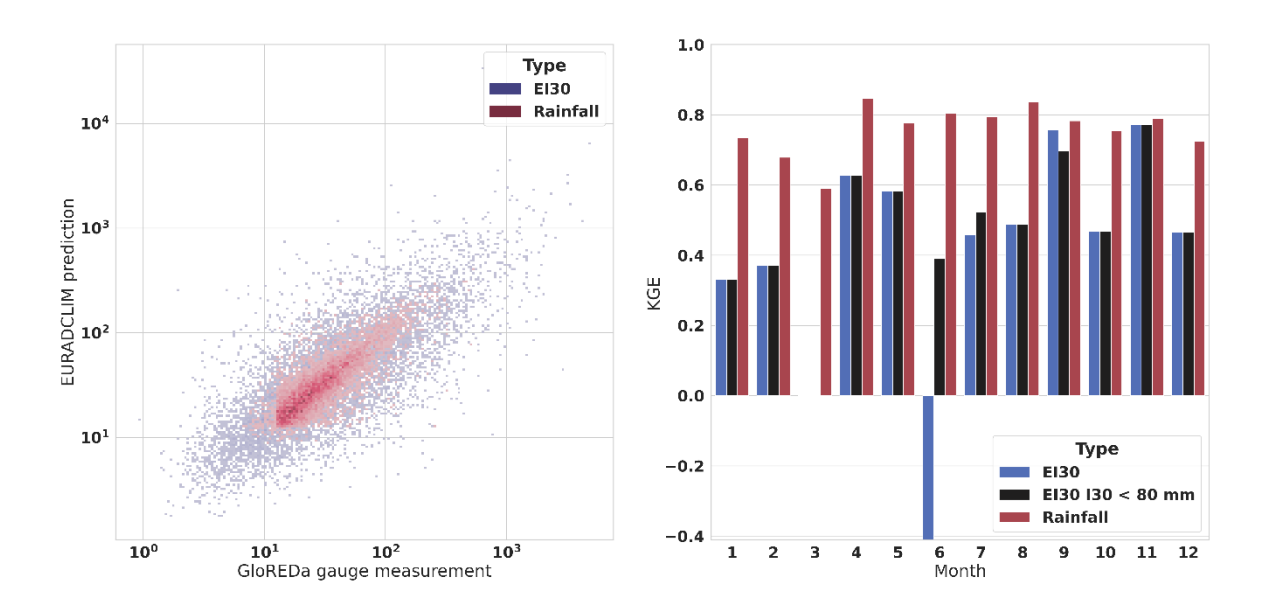


Figure S10: Left: Comparisons of predicted rainfall depth and EI30 from EURADCLIM against rain gauge measurements in Slovenia between 2016 and 2020. Right: Monthly evaluations of the predicted EI30 and rainfall depth via the Kling-Gupta index using an unlimited I30 (blue) and an I30 limited to 80 mm/h (black).

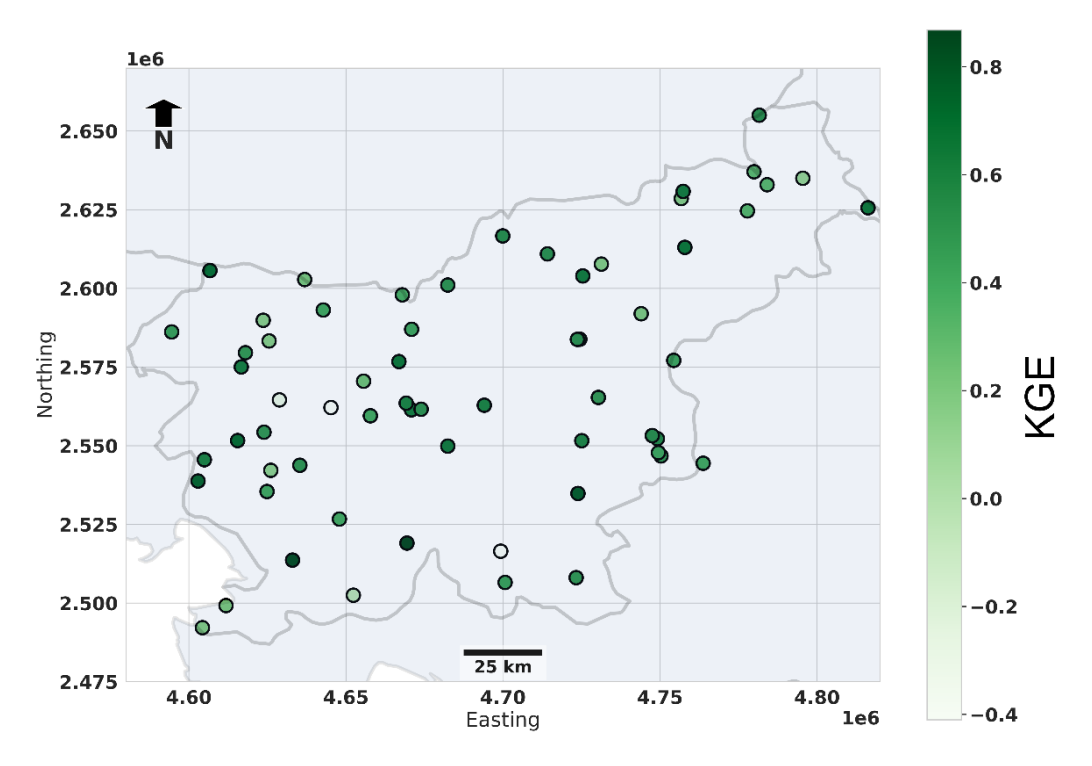


Figure S11: Location specific evaluations of EURADCLIM predictions of EI30 across Slovenia between 2016 and 2020. The KGE represents the Kling-Gupta Efficiency.

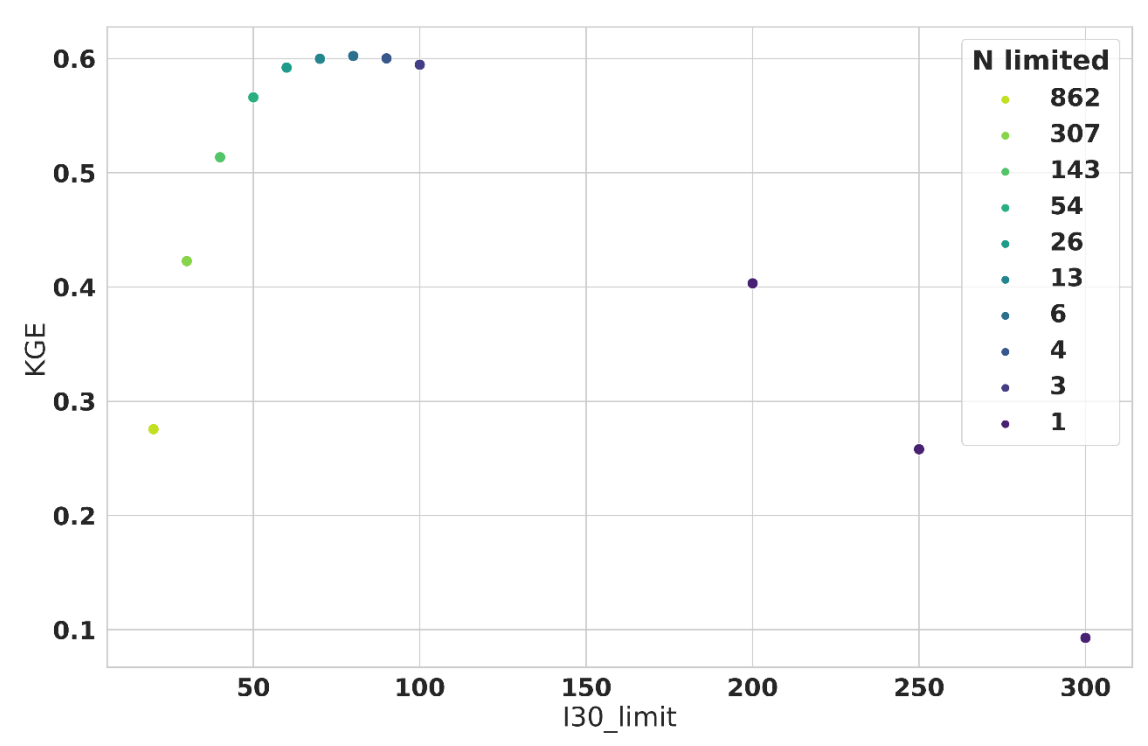


Figure S12: Comparison of impact of different I30 limit (mm/hr) values (I30\_limit) applied to the EURADCLIM-derived EI30 for the Slovenian stations included in the GloREDa for the 2016-2020 period. The points show the trend in the Kling-Gupta Efficiency (KGE) when differing limits were applied (i.e., the maximum permittable I30 value) in the calculation of EI30. "N limited" shows the number of EI30 events affected for each I30 limit, showing the changing number of impacted events when stricter limits are applied (i.e., lower maximum I30 values).

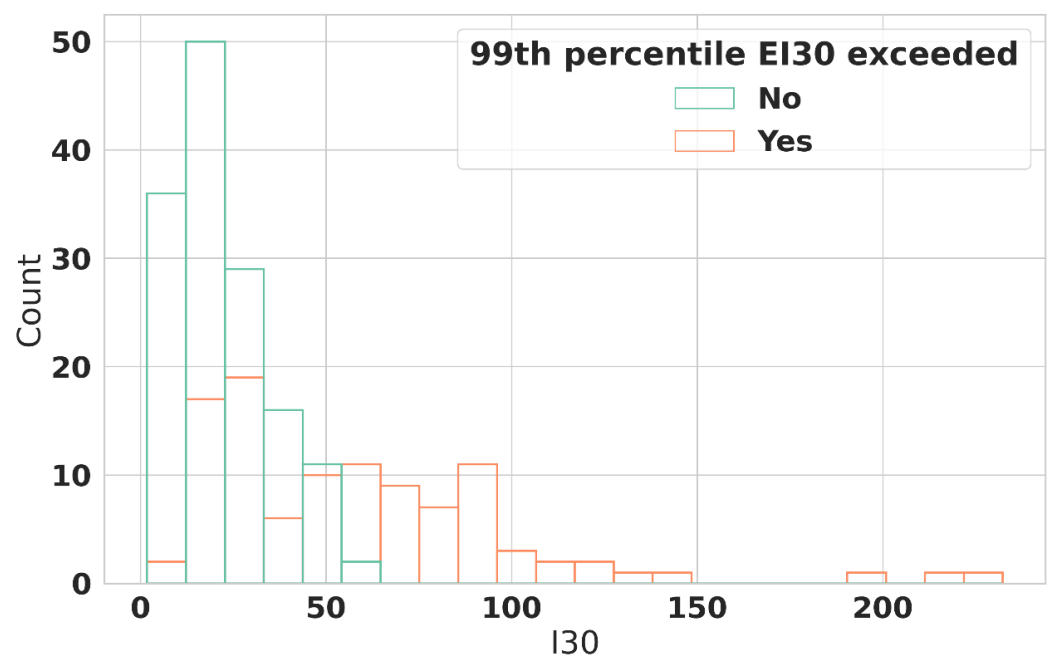


Figure S13: The populations of event-scale I30 (mm/hr) in which the  $99^{th}$  percentile EI30 value was exceeded by EURADCLIM (Yes) or not (No) compared to GloREDa. Each data point is generated based on the 99th percentile EI30 value in the population of events per country per month (i.e., 12 values per country). The histograms show the general separability of populations, in which overpredictions at high quantiles are characterised by unrealistic I30 values (e.g., > 60 mm/hr) derived from EURADCLIM which exceed the measured values in GloREDa.

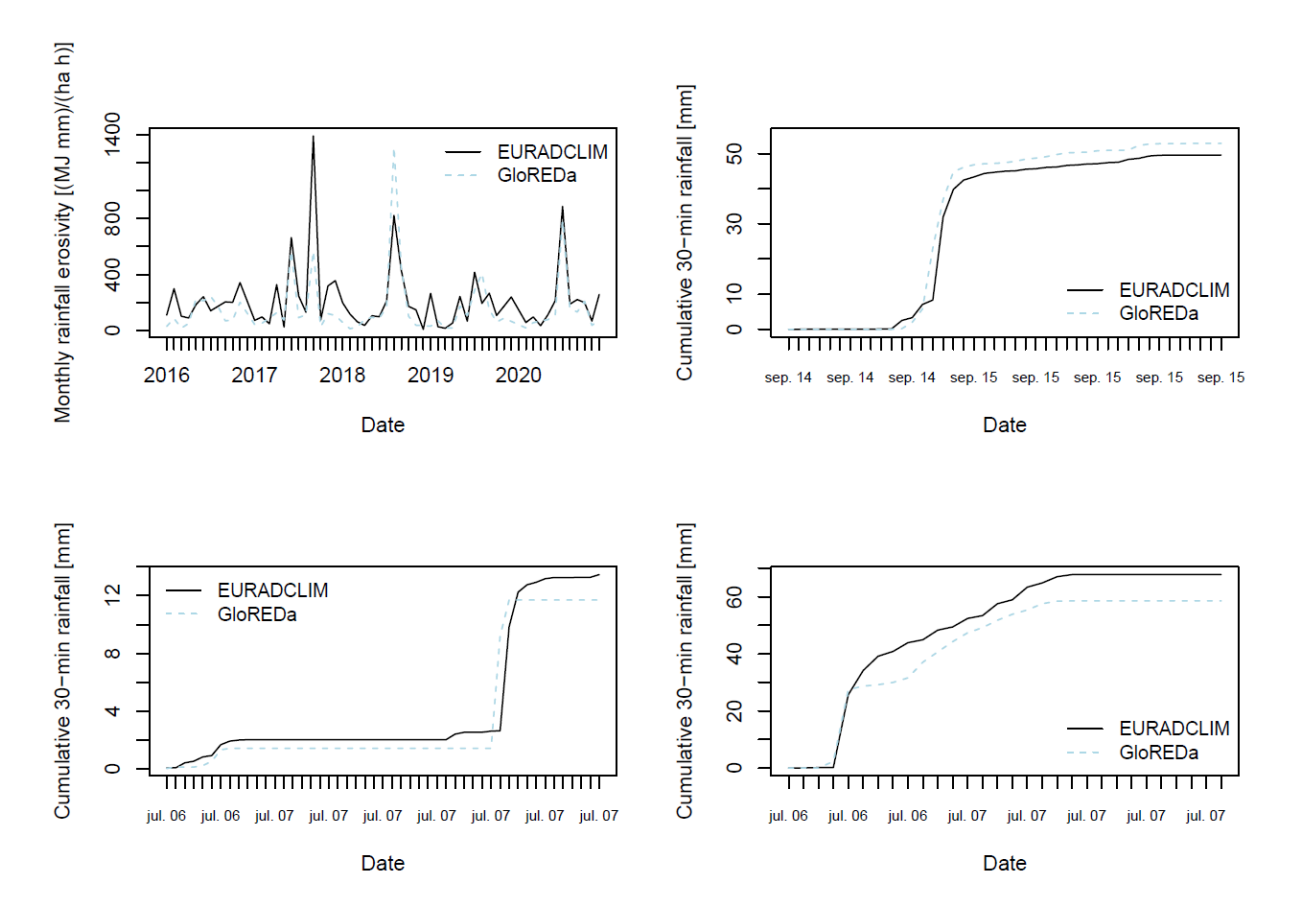


Figure S14: Comparison between monthly rainfall erosivity for 2016-2020 period calculated for the Ljubljana station (Slovenia) using EURADCLIM and GloREDa (top left) and comparison between cumulative 30-min rainfall between EURADCLIM and GloREDa for three specific rainfall events (i.e., 14.9.2017-top right, 6.7.2019-bottom left and 6.7.2020-bottom right).